

In vivo conversion of 18- and 20-C essential fatty acids in rats using the multiple simultaneous stable isotope method

Yu Hong Lin and Norman Salem, Jr.¹

Section of Nutritional Neuroscience, Laboratory of Membrane Biochemistry and Biophysics, National Institute on Alcohol Abuse and Alcoholism, National Institutes of Health, Bethesda, MD 20892-9410

Abstract An important question for mammalian nutrition is the relative efficiency of C18 versus C20 essential fatty acids (EFAs) for supporting the tissue composition of n-3 and n-6 pathway end products. One specific question is whether C22 EFAs are made available to tissues more effectively by dietary α -linolenic acid (18:3n-3) and linoleic acid (18:2n-6) or by dietary eicosapentaenoic acid (20:5n-3) and dihomo- γ -linolenic acid (20:3n-6). To address this question in a direct manner, four stable isotope compounds were given simultaneously in a novel paradigm. A single oral dose of a mixture of ²H₅-18:3n-3, ¹³C-U-20:5n-3, ¹³C-U-18:2n-6, and ²H₅-20:3n-6 was administered to rats given a defined diet. There was a preferential in vivo conversion of arachidonic acid (20:4n-6) to docosatetraenoic acid (22:4n-6) and of 22:4n-6 to n-6 docosapentaenoic acid (22:5n-6) when the substrates originated from the C18 precursors. However, when the end products docosahexaenoic acid (22:6n-3) or 22:5n-6 were expressed as the total amount in the plasma compartment divided by the dosage, this parameter was 11-fold greater for 20:5n-3 than for 18:3n-3 and 14-fold greater for 20:3n-6 than for 18:2n-6. Thus, on a per dosage basis, the total amounts of n-3 and n-6 end products accreted in plasma were considerably greater for C20 EFA precursors relative to C18.—Lin, Y. H., and N. Salem, Jr. *In vivo conversion of 18- and 20-C essential fatty acids in rats using the multiple simultaneous stable isotope method.* *J. Lipid Res.* 2005. 46: 1962–1973.

Supplementary key words stable isotope tracer • α -linolenic acid • eicosapentaenoic acid • docosahexaenoic acid • linoleic acid • dihomo- γ -linolenic acid • arachidonic acid • gas chromatography-mass spectrometry • multiple simultaneous stable isotopes

There have been many suggestions from tissue compositional studies that the rate-limiting step in essential fatty acid (EFA) biosynthesis is the Δ -6 desaturase step. For example, an increase in the dietary intake of linoleic acid (18:2n-6) up to 30 g/day (14% of calories) in humans in-

creased the 18:2n-6 level in blood but not that of its metabolites, dihomo- γ -linolenic acid (20:3n-6) and arachidonic acid (20:4n-6) (1–3), although this may also be attributable to saturation of the enzyme. In vitro studies of rat liver microsomes indicate that the Δ -6 desaturase has the lowest reaction rate of four metabolic steps in both the n-6 and n-3 pathways (4, 5). Both radioactive isotope and stable isotope tracer studies suggested that the rate-limiting step in n-6 pathways is from 18:2n-6 to γ -linolenic acid (18:3n-6) (6, 7). The limited Δ -6 desaturase activity apparent in these studies may have been in part the result of downregulation of this liver enzyme when diets containing higher levels of polyunsaturates are fed (8, 9).

20:3n-6 appears to be a more efficient substrate than its precursor 18:2n-6 for conversion to 20:4n-6 (10). el Boustani et al. (11, 12) first studied the conversion of ²H₄-20:3n-6 into ²H-20:4n-6 in human subjects and observed significant activity; this was later confirmed by Emken et al. (13). In contrast, 18:2n-6 appears to be relatively inefficiently converted to 20:4n-6. For example, Mohrhauer and Holman (14) observed that feeding 1.79 energy% 18:2n-6 produced a liver 20:4n-6 level of 9.6%, whereas feeding as little as 0.27 energy% preformed 20:4n-6 led to a 20:4n-6 content of >11%. Similarly, when the doses of supplemental α -linolenic acid (18:3n-3) and eicosapentaenoic acid (20:5n-3) are compared in various studies, it is apparent that dietary 20:5n-3 was more efficacious than 18:3n-3 in increasing 20:5n-3 and docosapentaenoic acid (22:5n-3) levels in

Abbreviations: 18:2n-6, linoleic acid; 18:3n-3, α -linolenic acid; 20:4n-6, arachidonic acid; 20:3n-6, dihomo- γ -linolenic acid; 22:6n-3, docosahexaenoic acid; 22:5n-6, n-6 docosapentaenoic acid; 20:5n-3, eicosapentaenoic acid; AUC, area under the curve; CE, cholesteryl ester; C_{max}, maximal concentration of labeled fatty acids in plasma; D_{max}, maximal percentage of dose; EFA, essential fatty acid; E_{max}, maximal enrichment of labeled fatty acids at maximal concentration; MESSI, multiple simultaneous stable isotope; PC, phosphatidylcholine; PE, phosphatidylethanolamine; PI, phosphatidylinositol; PL, phospholipid; TG, triglyceride; T_{max}, sampling time at maximal concentration.

¹ To whom correspondence should be addressed.

e-mail: nsalem@niaaa.nih.gov

Manuscript received 1 April 2005.

Published, JLR Papers in Press, June 1, 2005.

DOI 10.1194/jlr.M500127.JLR200

the human circulation (15–20). Neither was effective in increasing docosahexaenoic acid (22:6n-3, DHA) content in the human circulation.

Thus, the suggestion has been made that it is desirable to bypass this initial desaturase step in supplying precursor fatty acids in the diet to support the composition of the metabolic end products of the n-3 and n-6 pathways. This may be particularly important during early development, as, for example, 18:3n-6 or 20:3n-6 have been added to infant formula or artificial rat milk in place of 20:4n-6 (21, 22).

The purpose of this study was to evaluate the *in vivo* metabolism of dietary 18:3n-3 compared with that of 20:5n-3 and of dietary 18:2n-6 compared with that of 20:3n-6. We used stable isotope markers as pioneered by Emken and colleagues (23, 24) and used by several other groups for human (25–30) or nonhuman primate (31) stable isotope tracer studies of 18:2n-6 and 18:3n-3 metabolism. Here, we demonstrate that the direct longitudinal comparison of four isotopes is possible when given simultaneously to the same individual. This analytical technique has been described and termed multiple simultaneous stable isotopes (MESSI) (32). It uses several stable isotopic fatty acids given simultaneously and labeled with either deuterium or carbon-13 to yield isotopomers of differing mass values, which can then be independently measured with a highly sensitive, negative chemical ionization gas chromatography-mass spectrometry measurement technique. This approach has the advantage that identical experimental conditions are used for each isotopic fatty acid to be compared as they are metabolized in the same animals at the same time.

MATERIALS AND METHODS

Animals and diet

This study was performed after a protocol was approved by the National Institute on Alcohol Abuse and Alcoholism Animal Care and Use Committee, National Institutes of Health. Three week old, weaning male Sprague-Dawley rats (murine pathogen-free; Taconic, Germantown, NY) were purchased and group housed in our animal facility under conventional conditions. The animal holding facility had a 12 h (7 AM to 7 PM) light cycle, a temperature of 22°C, and a relative humidity of ~55%. Rats were fed pelleted food and water *ad libitum* with a custom diet (custom diet 100509; Dyets, Bethlehem, PA) based on the AIN-93G (33) standard as detailed in **Table 1**. The diet was modified with respect to its fat components to yield a fatty acyl distribution of 40% saturated fat, 42% monounsaturates, 15% 18:2n-6, and 3% 18:3n-3; no longer chain (C20 and C22) EFAs were added to the fat mixture.

After maintenance on this diet for 9 weeks, average body weights were 418 ± 37 g. One day before the start of the experiment, seven rats were singly housed, fasted for 12 h (2 PM to 2 AM), and then allowed their day's ration of food over a 5 h period. A mean weight of 9.3 ± 1.7 g of food (containing ~28 mg of 18:3n-3 and 140 mg of 18:2n-6) was consumed during this time. Rats were then dosed with an ethyl ester mixture of 32 μmol of $^2\text{H}_5$ -18:3n-3, 2.9 μmol of ^{13}C -20:5n-3, 155 μmol of ^{13}C -18:2n-6, and 2.1 μmol of $^2\text{H}_5$ -20:3n-6 in olive oil in a total of 0.4 ml and returned to their home cages. The dosing was done by gavage using a 16 gauge, 3 inch long animal feeding needle attached to a 1 ml syringe. An aliquot of the isotope mixture was saved for quantitative fatty

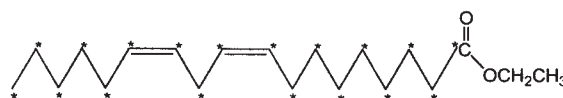
acid analysis. Animals were then given access to food 4 h after dosing and maintained for 30 days with *ad libitum* access to the custom diet and water.

Stable isotopes

Scheme 1: Deuterated α -linolenate ethyl ester (17,17,18,18,18- $^2\text{H}_5$ -18:3n-3; $^2\text{H} > 95\%$), **Scheme 2:** carbon-13-uniformly labeled linoleate ethyl ester (^{13}C -U-18:2n-6; $^{13}\text{C} > 95\%$), and **Scheme 3:** deuterated 20:3n-6 ethyl ester (19,19, 20,20,20- $^2\text{H}_5$ -20:3n-6; $^2\text{H} > 95\%$) were obtained from Cambridge Isotope Laboratories (Andover, MA); **Scheme 4:** carbon-13-uniformly labeled eicosapentaenoate ethyl ester (^{13}C -U-20:5n-3; $^{13}\text{C} > 95\%$) was obtained from Martek Bioscience Corp. (Columbia, MD). All isotopes were repurified by HPLC and were of 95–99% chemical purity as assessed by GC, GC-MS, and NMR analyses. The structures of the four stable isotope-labeled fatty acids are shown below (asterisks indicate either deuterium or carbon-13 atoms).



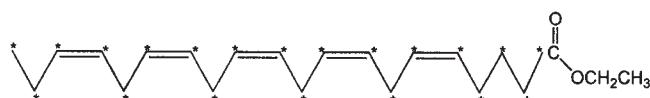
Scheme 1



Scheme 2



Scheme 3



Scheme 4

All solvents were of gas chromatographic or higher grade except acetonitrile, which was HPLC grade. Other chemicals were of analytical-reagent grade. They were commercially purchased and used without further purification.

Repeated blood sampling from the rat caudal lateral vein

To habituate the rats to the Plexiglas restraint cylinder to be used for blood collection, animals were placed in the chamber for 2 min/day over a 10 day period before the start of the experiment. To achieve vasodilation to promote bleeding, animals were placed on a warm water bottle and their tails placed into water at 50°C for ~1 s before sampling, and then gentle massage was applied to the tail to aid in blood flow. Blood (0.1–0.2 ml/sample) was then collected using a heparinized 23 gauge, 1 inch long needle (without adaptor) via lateral vein puncture as described (34). Skilled personnel could withdraw 0.2 ml of blood in ~1 min. Sampling started from the distal end of the tail and then gradually moved forward with alternative sampling of first the right and then the left lateral veins, so that the same puncture

TABLE 1. Nutrient composition of the experimental diet^a

Ingredient	Amount	Ingredient	Amount
	<i>g/kg diet</i>		<i>g/kg diet</i>
Protein		Other	
Casein, vitamin-free	200	Cellulose	50
Carbohydrate		Mineral and salt mix	35
Cornstarch	150	Vitamin mix	10
Dextrose	199	L-Cystine	3
Maltose-dextrin	150	Choline bitartrate	2.5
Sucrose	100	<i>tert</i> -Butyl-hydroquinone	0.02
Fat			
Hydrogenated coconut oil	29.7		
Olive oil	52.2		
Safflower oil	13		
Flaxseed oil	5.1		
Fatty Acid Composition ^b		Percentage of Total Fatty Acids	
Saturates		40	
Monounsaturates		42	
18:2n-6		15	
18:3n-3		3	

^a The experimental diet was a modification of the AIN-93G (33) formulation from Dyets.

^b C20 and C22 polyunsaturates occurred only at trace levels.

site was not used twice. Water was supplied ad libitum, and normal saline was given periodically during the first week of the experiment, particularly during the first 36 h after dosing. This sampling technique caused no tail necrosis during the entire 30 day experimental period.

A total of 24 blood samples were collected after dosing with the four isotopes at the following time points: 1, 2, 4, 6, 8, 16, 24, 36, 48, 60, 72, 84, 96, 108, 120, 132, 144, and 168 h and 11, 14, 18, 23, 27, and 30 days. Baseline samples were taken 1 day before dosing. One control animal gavaged with olive oil was periodically sampled to confirm that the olive oil vehicle did not alter the baseline for the various GC-MS signals to be measured. Blood samples were kept on melting ice and then centrifuged in 1.5 ml Eppendorf tubes for 10 min at 1,250 *g*. Plasma was removed, quickly frozen using dry ice, and then stored at -80°C until analysis.

Total lipid extraction, derivatization reactions, and instrumental conditions

Both labeled exogenous fatty acids and endogenous fatty acids were analyzed in each plasma sample at every time point by GC-MS in negative chemical ionization analysis (32, 35, 36) and gas chromatography-flame ionization detection (36, 37), respectively, as described previously. Calibrations were performed for these mass spectral data as described in the accompanying paper (36).

Data analysis and calibration

The unlabeled fatty acid values in the samples were calculated by comparing the integrated areas of the fatty acid peaks on the gas chromatograms with that of the internal standard. Fatty acid weights were converted to moles using the respective molecular weights for each compound. Data are expressed as means \pm SEM ($n = 7$) as nanomoles of fatty acid per milliliter of plasma.

To express mass spectral data in terms of nanomoles, the peak areas of each labeled compound as detected by selected ion monitoring were compared with that of the internal standard. The standard curves for the various compounds were able to calibrate a range of sample amount loaded onto the GC column from ~ 0.003 to 1.7 pmol. This process is described in detail in the accompanying paper for $^2\text{H}_5$ -18:3n-3, ^{13}C -U-18:2n-6, ^{13}C -U-20:5n-3, and $^2\text{H}_5$ -20:3n-6 standard curves presented (36). The calibration curves for the in vivo metabolites from the four precursors were

derived from those made with the isotopic precursors and unlabeled EFAs.

The maximal concentration (C_{max}) and time point of the maximal concentration (T_{max}) for each labeled fatty acid in plasma was obtained directly from the concentration-time course curves. The half-time corresponded to the time that the plasma concentration decreased to half its maximal value, C_{max} , on the concentration-time course curve. The maximal percentage of dose (D_{max}) expresses the percentage of the oral isotopic dose observed in plasma, and it was calculated as follows: $[C_{\text{max}} \times \text{total plasma volume} \times \text{dose}^{-1}] \times 100$. The maximal enrichments (E_{max}) were calculated at these time points by dividing the concentration of the stable isotope-labeled compound of interest by the concentration of the unlabeled endogenous compound. Area under the curve (AUC) was calculated using a trapezoidal method starting from 0 h, with the curve drawn between each succeeding time point until such time as the signal could no longer be reliably detected (38–40). A two-sided, pairwise Student's *t*-test was applied to detect significant differences ($P < 0.05$) using Excel 2002 for Windows 2000 Professional (Microsoft, Seattle, WA).

RESULTS

Diets and animals

To have a well-defined metabolic experiment involving fatty acids, the diet must be carefully controlled, particularly with respect to its EFA content. In this study, a semi-synthetic diet was used based on the AIN-93G standard (33). The macronutrients of protein, carbohydrate, and fat represented ~ 19 , 56, and 23% of calories, respectively. The fat content was 10 wt% and was constructed to supply $\sim 15\%$ of the fatty acids as 18:2n-6 and 3% as 18:3n-3 to produce a 5:1 ratio of n-6/n-3 fatty acids (Table 1). The remainder was composed of approximately equal amounts of saturated and monounsaturated fatty acids. Animals were allowed to equilibrate their tissue lipid composition with this diet for 9 weeks before the experiment.

Adult male rats 12 weeks of age with a mean body weight of 418 ± 37 g were used. After dosing of the stable isotope mixture and frequent blood sampling, the mean body weights of the rats declined within the first 24 h by 4.7 ± 0.4 g. Accurate sampling times were maintained throughout the study with a coefficient of variation of $<5\%$ over the first 36 h and $<0.5\%$ thereafter.

Multiple ion chromatograms

To demonstrate that the multiple isotope tracer technique used here is valid, selected ion chromatograms are presented for some of the principal metabolites (Fig. 1). It is demonstrated that for each metabolite, the endogenous (unlabeled), deuterium-labeled, and carbon-13-labeled compounds of the same fatty acid can be independently measured in the same animal. For example, in Fig. 1A, the endogenous 22:5n-3 was detected at the M-PFB mass value of 329; this peak is enormous compared with the trace signals representing the stable isotope-labeled metabolites. The ^{13}C -22:5n-3 is not chromatographically resolved from the endogenous 22:5n-3 but has an m/z value of 349; thus, the mass spectrometer can easily detect this as a discrete signal unaffected by the large endogenous signal at m/z 329. The deuterium-labeled 22:5n-3 is baseline separated from the endogenous 22:5n-3 peak envelope because of the presence of five deuterium atoms (by 0.25 min); thus, its signal at m/z 334 is easily resolved from either of the other two 22:5n-3 species. Similarly, the three selected ion chromatograms are presented in Fig. 1B–F for the endogenous, ^{13}C - and $^2\text{H}_5$ -derived signals for 22:6n-3, 24:5n-3, 24:6n-3, 22:4n-6, and 22:5n-6. From these plots, it can be observed that the signal abundances of C22 n-3 PUFAs were ~ 1 order of magnitude greater (1,000–3,000 counts; Fig. 1A, B) than those of the C22 n-6 PUFAs (100–400 counts; Fig. 1E, F) at the dosages given as a result of the larger isotopic dilutions of the n-6 precursors from the endogenous pools relative to those of the n-3 precursors.

Time course curves of the four precursors

A sufficient number of time points during sampling of the plasma were obtained to provide a good description of the in vivo absorption, decay, and elimination phases of the concentration-time course curves of the four precursors (Fig. 2). The four isotopic precursors and the symbols used to denote them both in the text and in the figures are as follows: $^2\text{H}_5$ -18:3n-3 (open triangles), ^{13}C -U-20:5n-3 (open circles), ^{13}C -U-18:2n-6 (closed triangles), and $^2\text{H}_5$ -20:3n-6 (closed circles). Larger doses of the C18 isotopes were given relative to the C20 isotopes, so the C20 isotopes are plotted on a separate y axis scale appearing on the right. Three precursors, ^{13}C -U-20:5n-3, ^{13}C -U-18:2n-6, and $^2\text{H}_5$ -20:3n-6, shared a similar kinetic appearance, reaching C_{max} values of 7.7 ± 1.5 , 102 ± 11 , and 3.2 ± 0.5 nmol/ml, respectively, at 6.45 ± 0.05 h, as seen in Table 2. Continued metabolism then decreased the isotopomer concentrations to half of the C_{max} value in 7, 8, and 9 h, respectively. The precursors were still detectable in plasma at 60 h after dosing. In contrast, the $^2\text{H}_5$ -18:3n-3 reached its C_{max} of 14 ± 3 nmol/ml at a T_{max} of 1.2 ± 0.02 h. The isotopomer con-

centration then decreased to half of the C_{max} in ~ 5 h, and it nearly disappeared from plasma by 36 h.

D_{max} values, describing the maximal percentage of the initial dose in the plasma compartment, were as follows: $0.7 \pm 0.1\%$ for 32 μmol of 18:3n-3, $4.1 \pm 0.7\%$ for 2.9 μmol of 20:5n-3, $1.0 \pm 0.1\%$ for 155 μmol of 18:2n-6, and $2.3 \pm 0.3\%$ for 2.1 μmol of 20:3n-6 (Table 2). Thus, the C20 precursors showed greater entry into rat plasma per milligram of administered dosage compared with the C18 precursors. Different dosages for the various precursors were administered in an attempt to compensate for likely differences in the endogenous pool sizes maintained by the combined interactions of a steady daily dietary input with the inherent metabolic dynamics. E_{max} values for the four precursors appearing in plasma had a small range (10.4, 11.4, 18.5, and 19.2; Table 2), indicating a relatively successful choice of comparable dietary doses. Following the first metabolic step after the C20 precursors, Table 2 shows that E_{max} values for the two isotopomers were similar for 20:4n-6 (0.169 and 0.225) in the n-6 pathway and for 22:5n-3 (2.93 and 3.51) in the n-3 pathway. However, the lower subsequent enrichment of n-6 metabolites compared with n-3 metabolites likely reflects the relatively large pools of tissue 20:4n-6 that are maintained by the steady daily dietary intake of ~ 300 mg of 18:2n-6.

Metabolite concentration-time course curves

The various n-3 metabolites of the stable isotope-labeled precursors are presented in Fig. 3. In Fig. 3A, the concentration of the ^{13}C -U-20:5n-3 precursor is depicted along with the smaller amounts of $^2\text{H}_5$ -20:5n-3 formed from $^2\text{H}_5$ -18:3n-3. The concentrations of the two isotopomers are similar after one elongation step had occurred, with the production of 22:5n-3, with only a slightly greater peak concentration of the ^{13}C -labeled isotopomer formed from ^{13}C -20:5n-3 (Fig. 3B, Table 2). Much lower concentrations ($C_{\text{max}} = 10$ –27 pmol/ml) of the C24 metabolites were observed in plasma relative to 22:5n-3 and 22:6n-3 (C_{max} near 1,000 pmol/ml). Nevertheless, as n-3 metabolism proceeded by elongation to 24:5n-3, desaturation to 24:6n-3, and retroconversion to 22:6n-3, there was a continued slight predominance of the ^{13}C -labeled compounds relative to the ^2H -labeled compounds (Fig. 3C–E). The different turnover rates of isotopomers in the different metabolite pools can be described by the time to decrease peak concentrations by half ($T_{\text{Cl}/2}$). Such half-time values (in hours) were for 18:3n-3 (5), 20:3n-3 (5), 20:4n-3 (5), 20:5n-3 (14 vs. 7), 22:5n-3 (29 vs. 27), 24:5n-3 (24 vs. 22), 24:6n-3 (32 vs. 26), 22:6n-3 (90 vs. 84) of ^2H -18:3n-3-derived vs. ^{13}C -20:5n-3-derived isotopomers. E_{max} values indicate only slightly greater enrichment for the ^{13}C -labeled compounds derived from dietary 18:3n-3 relative to the ^2H -labeled products from 20:5n-3 (Table 2), even though the initial dietary dose was 10-fold greater.

The metabolism of the two n-6 isotopes to 20:3, 20:4, 22:4, and 22:5 are shown in Fig. 4. Here again, the newly added isotope, $^2\text{H}_5$ -20:3n-6, was 3-fold more abundant than that formed from ^{13}C -18:2n-6 (Fig. 4A), even though the C18 dietary precursor was added at a >50 -fold amount. However, for the first metabolite of 20:3n-6, the Δ -5 desat-

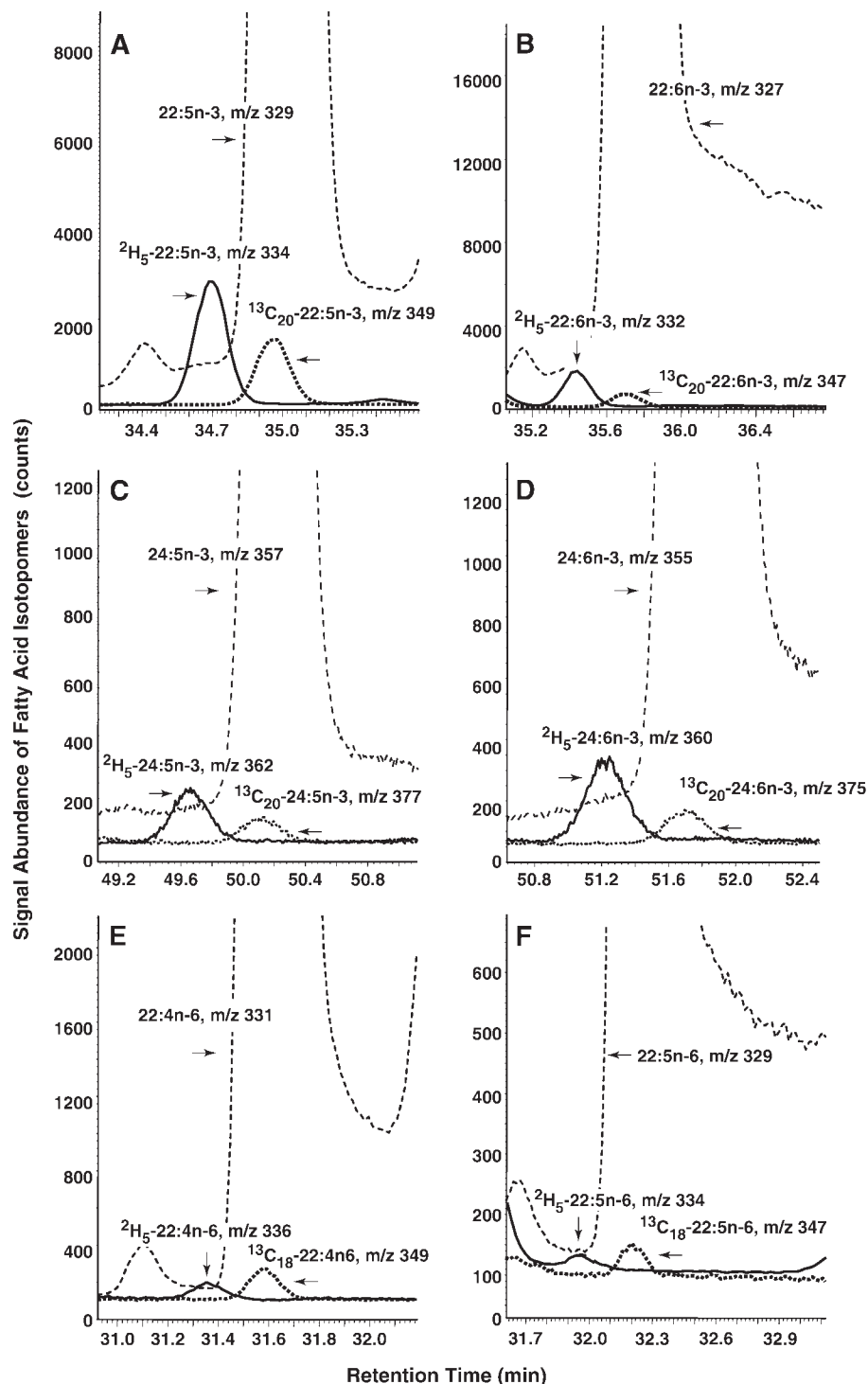


Fig. 1. Selected ion chromatograms of fatty acid pentafluorobenzyl esters in the selected ion monitoring mode of negative chemical ionization GC-MS analysis showing signal abundances (counts) of each ion (M-PFB). $^2\text{H}_5$ (solid lines) and ^{13}C (dotted lines) isotopomers of C22 and C24 essential fatty acids desaturated and elongated from stable isotope-labeled C18 and C20 precursors are plotted along with their respective unlabeled endogenous forms (dashed lines). Results shown are for fatty acids after the administration of the mixture of $^2\text{H}_5$ -18:3n-3, ^{13}C -U-20:5n-3, ^{13}C -U-18:2n-6, and $^2\text{H}_5$ -20:3n-6. Ion chromatograms are shown for each fatty acid metabolite during a period when the responses are close to maximal. A: 22:5n-3 at 12 h. B: 22:6n-3 at 12 h. C: 24:5n-3 at 12 h. D: 24:6n-3 at 12 h. E: 22:4n-6 at 60 h. F: 22:5n-6 at 60 h.

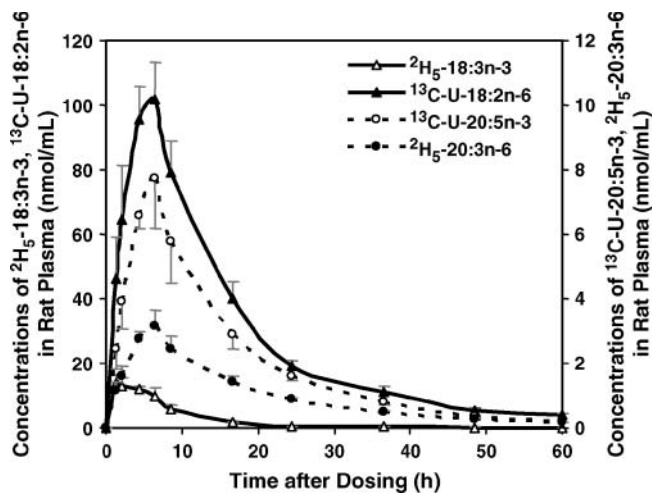


Fig. 2. Time course curves of the concentrations (nmol/ml plasma) of the labeled fatty acid precursors $^{13}\text{C-U-18:2n-6}$ (closed triangles), $^2\text{H}_5\text{-20:3n-6}$ (closed circles), $^2\text{H}_5\text{-18:3n-3}$ (open triangles), and $^{13}\text{C-U-20:5n-3}$ (open circles) in rat plasma as a function of time over 60 h after a single dosing. Concentrations of the C20 precursors are shown on the right y axis. Values are expressed as means \pm SEM ($n = 7$).

urated 20:4n-6 (Fig. 4B), and for subsequent metabolites (Fig. 4C, E), the isotopomer originating from dietary $^{13}\text{C-U-18:2n-6}$ was a relatively greater contributor than dietary $^2\text{H}_5\text{-20:3n-6}$. The conversion of 20:3n-6 to 20:4n-6 had an apparently greater accumulation of isotope from ^{13}C -labeled 20:3n-6 (C_{max} from 1.12 to 3.24) but a lower accumulation from ^2H -labeled 20:3n-6 (C_{max} from 3.17 to 2.22).

The different half-times in the various metabolite pools expressed as $T_{\text{Cl}/2}$ values (in hours) were for 18:2n-6 (8), 18:3n-6 (24), 20:3n-6 (31 vs. 9), 20:4n-6 (144 vs. 84), 22:4n-6

(224 vs. 204), 24:5n-6 (>168 vs. 144), and 22:5n-6 (190 vs. 110) for $^{13}\text{C-18:2n-6}$ -derived vs. $^2\text{H-20:3n-6}$ -derived isotopomers. Longer half-time values likely occur with the larger pools of n-6 metabolites in tissues compared with n-3 metabolites from a less abundant dietary source. E_{max} values showed only a several-fold greater enrichment for ^{13}C - compared with ^2H -isotopomers, even though the dietary ^{13}C -precursor dose was >50-fold greater than that of the ^2H -labeled C20 precursor (Table 2). For the n-6 fatty acids, the C24 signals were weak and variable, and time course curves could not be reliably obtained for 24:4n-6 at this low level of isotopic tracer. During the formation of 24:5n-6 (Fig. 4D), the proportions of the ^{13}C -isotopomers appeared to be 5-fold greater than those of the ^2H -isotopomers, in contrast to the observed 2-fold greater proportion observed for 22:4n-6 (Fig. 4C) and the 4-fold greater proportion seen for 22:5n-6 (Fig. 4E). Labeled 20:4n-6 and its metabolites, 22:4n-6 and 22:5n-6, appeared to be relatively long-lived (half-time values of 100–200 h), as also indicated by their detection at the end of the 30 day experiment. The prolonged presence would likely be enhanced by the steady entry of isotopomers from the abundant tissue pools of 20:3n-6 isotopomers.

The ratios of C_{max} values for isotopomers of ^{13}C -labeled to ^2H -labeled 20:4n-6 (1.5), 22:4n-6 (3.1), and 22:5n-6 (4.6) showed a progressively greater tendency ($P < 0.05$) toward more metabolites being formed from the $^{13}\text{C-U-18:2n-6}$ precursor than from the $^2\text{H}_5\text{-20:3n-6}$ precursor. However, no progressive difference was observed for the ratios of isotopomers of 22:5n-3 and 22:6n-3 in this study.

The general temporal relationships of isotope appearance among the various fatty acids in plasma were as expected if the metabolic scheme of Voss et al. (41) is as

TABLE 2. Maximal values of ^2H - and ^{13}C -labeled fatty acids in rat plasma after dosing with $^2\text{H}_5\text{-18:3n-3}$, $^{13}\text{C-U-20:5n-3}$, $^{13}\text{C-U-18:2n-6}$, and $^2\text{H}_5\text{-20:3n-6}$

Fatty Acids	C_{max}		D_{max}		E_{max}		T_{max}	
	^2H	^{13}C	^2H	^{13}C	^2H	^{13}C	^2H	^{13}C
	nmol/ml plasma		% of dose/plasma compartment		nmol/nmol%		h	
n-3								
18:3n-3	13.8 \pm 2.7	— ^a	0.672 \pm 0.139	—	18.5 \pm 3.2	—	1.24 \pm 0.02	—
20:3n-3	0.169 \pm 0.033	—	0.008 \pm 0.002	—	13.9 \pm 1.1	—	6.35 \pm 0.05	—
20:4n-3	0.164 \pm 0.031	—	0.008 \pm 0.001	—	12.9 \pm 2.5	—	6.35 \pm 0.05	—
20:5n-3	1.99 \pm 0.18	7.73 \pm 1.54^b	0.095 \pm 0.007	4.12 \pm 0.74^b	4.77 \pm 0.31	19.2 \pm 4.0^b	6.35 \pm 0.05	6.35 \pm 0.05
22:5n-3	1.06 \pm 0.05	1.28 \pm 0.18	0.051 \pm 0.004	0.693 \pm 0.09 ^b	2.93 \pm 0.08	3.51 \pm 0.42	8.55 \pm 0.15	8.55 \pm 0.15
24:5n-3	0.010 \pm 0.002	0.015 \pm 0.003 ^b	0.0005 \pm 0.0001	0.008 \pm 0.002 ^b	2.23 \pm 0.2	3.14 \pm 0.39 ^b	16.6 \pm 0.1	16.6 \pm 0.1
24:6n-3	0.020 \pm 0.004	0.027 \pm 0.006	0.001 \pm 0.0002	0.015 \pm 0.004 ^b	1.13 \pm 0.08	1.46 \pm 0.20	24.4 \pm 0.1	24.4 \pm 0.1
22:6n-3	0.984 \pm 0.103	1.04 \pm 0.12	0.047 \pm 0.005	0.563 \pm 0.068 ^b	0.511 \pm 0.052	0.54 \pm 0.06	24.4 \pm 0.1	24.4 \pm 0.1
n-6								
18:2n-6	0.069 \pm 0.016 ^c	102 \pm 11	0.049 \pm 0.01	1.01 \pm 0.10	0.008 \pm 0.001	11.4 \pm 1.0	6.35 \pm 0.05	6.35 \pm 0.05
18:3n-6	0.025 \pm 0.006 ^c	0.437 \pm 0.037	0.018 \pm 0.004	0.004 \pm 0.0003	0.325 \pm 0.123	5.16 \pm 0.77	6.35 \pm 0.05	6.35 \pm 0.05
20:2n-6	—	0.34 \pm 0.066	—	0.003 \pm 0.001	—	5.30 \pm 0.84	—	16.6 \pm 0.1
20:3n-6	3.17 \pm 0.48	1.12 \pm 0.08 ^b	2.27 \pm 0.30	0.011 \pm 0.001 ^b	10.4 \pm 2.5	3.54 \pm 0.38 ^b	6.35 \pm 0.05	8.55 \pm 0.15 ^b
20:4n-6	2.22 \pm 0.36	3.24 \pm 0.49 ^b	1.59 \pm 0.23	0.032 \pm 0.004 ^b	0.169 \pm 0.026	0.25 \pm 0.04 ^b	24.4 \pm 0.1	36.6 \pm 0.1 ^b
22:4n-6	0.015 \pm 0.002	0.044 \pm 0.007 ^b	0.011 \pm 0.002	0.0005 \pm 0.0001 ^b	0.118 \pm 0.017	—	36.6 \pm 0.1	36.6 \pm 0.1
24:5n-6	0.0003 \pm 0.00004	0.002 \pm 0.0002	0.0002 \pm 0.00002	0.00002 \pm 0.000003	0.085 \pm 0.017	—	48.5 \pm 0.1	48.5 \pm 0.1
22:5n-6	0.003 \pm 0.0004	0.015 \pm 0.002 ^b	0.0024 \pm 0.0003	0.00015 \pm 0.00003 ^b	0.022 \pm 0.004	0.10 \pm 0.01 ^b	60.1 \pm 0.1	60.1 \pm 0.1

C_{max} , maximal concentration; D_{max} , percentage of maximal amount out of oral dosages in each animal; E_{max} , maximal enrichment; T_{max} , time point at the maximal concentration. The maximal values are expressed as means \pm SEM for seven animals, except for 24:5n-6 values ($n = 3$). Values in boldface type are the stable isotope labeled compounds given.

^a A dash indicates that the data were not available because of a nondetectable signal or a high baseline.

^b Significantly different from the corresponding deuterium-labeled compound ($P < 0.05$).

^c Indicates retroconversion from $^2\text{H}_5\text{-20:3n-6}$.

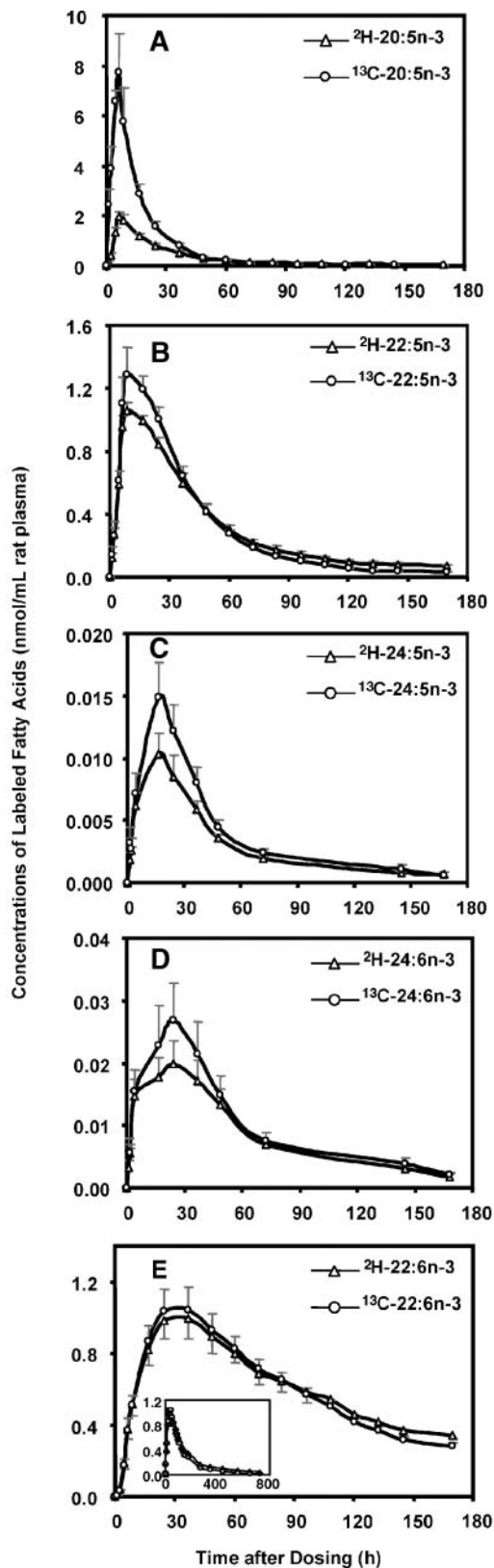


Fig. 3. Comparison of the time course-concentration (nmol/mL plasma) curves for the n-3 polyunsaturates in rat plasma for the ^2H (open triangles) and ^{13}C (open circles) isotopomers of 20:5n-3 (A), 22:5n-3 (B), 24:5n-3 (C), 24:6n-3 (D), and 22:6n-3 (E) from 0 to 168 h after dosing with a mixture of $^2\text{H}_5$ -18:3n-3, ^{13}C -U-20:5n-3, ^{13}C -U-18:2n-6, and $^2\text{H}_5$ -20:3n-6. For 22:6n-3 isotopomers, time courses to 30 days are shown in the inset graph in E. Values are expressed as means \pm SEM (n = 7).

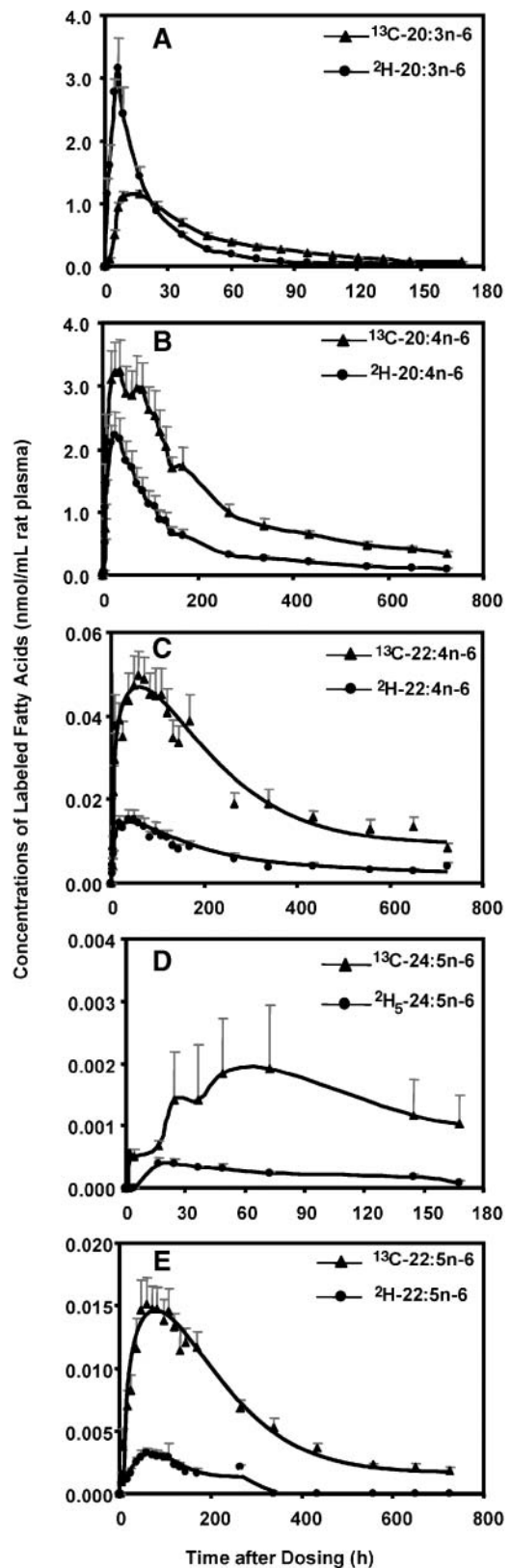


Fig. 4. Comparison of the time course-concentration (nmol/mL plasma) curves for the n-6 polyunsaturates in rat plasma for the ^2H (closed circles) and ^{13}C (closed triangles) isotopomers of 20:3n-6 (A) to 168 h (n = 7), 20:4n-6 (B) to 30 days (n = 7), 22:4n-6 (C) to 30 days (n = 7), 24:5n-6 (D) to 168 h (n = 3), and 22:5n-6 (E) to 30 days (n = 7) after dosing with a mixture of $^2\text{H}_5$ -18:3n-3, ^{13}C -U-20:5n-3, ^{13}C -U-18:2n-6, and $^2\text{H}_5$ -20:3n-6. Values are expressed as means \pm SEM.

sumed. C_{\max} values of the 18:3n-3, 20:5n-3, 22:5n-3, 24:5n-3, 24:6n-3, and 22:6n-3 isotopes were reached at 1.2, 6.4, 8.6, 16.6, 24.4, and 24.4 h, respectively (T_{\max} ; Table 2). This is consistent with the sequence of reactions in which the C24 pentaene and hexaene are precursors for 22:6n-3. Similarly, for the n-6 pathway, the isotopically labeled 18:2n-6, 20:3n-6, 20:4n-6, 22:4n-6, 24:5n-6 and 22:5n-6 reached their C_{\max} values at 6.4, 8.6, 36.6, 36.6, 48.5, and 60.1 h, respectively (T_{\max} ; Table 2).

Retroconversion

For the n-6 pathway, retroconversion of $^2\text{H}_5$ -20:3n-6 was apparent, as deuterium label could be detected in both 18:3n-6 and 18:2n-6. The time course curve of the concentrations of each of these fatty acids in plasma indicates a very rapid formation and accumulation of labeled 18:2 during the initial period, when the absorbed $^2\text{H}_5$ -20:3n-6 was well enriched in tissue pools (Fig. 5). The retroconverted 18:2n-6 and 18:3n-6 accounted for 2.2% and 0.8%, respectively, of the $^2\text{H}_5$ -20:3n-6, based upon a comparison of their C_{\max} in plasma. Interfering signals at the mass of $^{13}\text{C}_{18}$ -18:3n-3, $^{13}\text{C}_{20}$ -20:3n-3, and $^{13}\text{C}_{20}$ -20:4n-3 obviated the analysis of the retroconversion of ^{13}C -20:5n-3.

Integrated time-concentration curves

One measure of the apparent accumulation of labeled fatty acids in plasma over the entire experimental period (up to 30 d) is the AUC. This parameter is influenced by both the accretion of the particular metabolite and the persistence of that metabolite in the plasma. There is a significant difference ($P < 0.05$) between the AUC for the two isotopomers of 20:5n-3, with that of the ^{13}C -20:5n-3 being greater (Fig. 6A). However, there was no significant difference between the two 22:5n-3 or 22:6n-3 isotopomer values. Both isotopomers of 22:6n-3 showed higher AUC values than those of 22:5n-3 because of their more extended time course curves, which result from greater persistence in the plasma. A pattern distinct from that for n-3

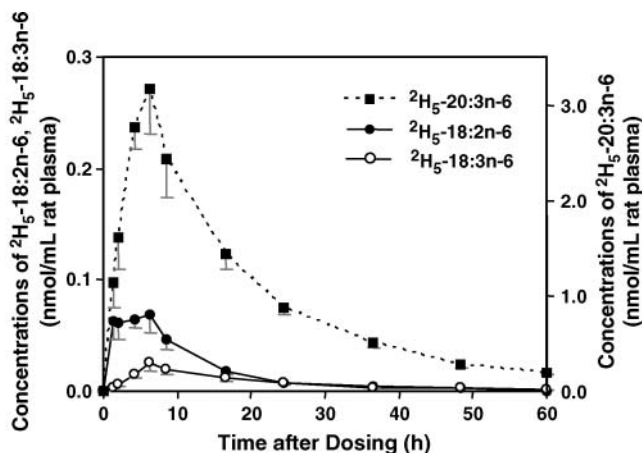


Fig. 5. In vivo retroconversion of $^2\text{H}_5$ -20:3n-6 (closed squares; right y axis) to $^2\text{H}_5$ -18:2n-6 (closed circles) and $^2\text{H}_5$ -18:3n-6 (open circles; left y axis) as reflected in rat plasma. Values are expressed as means \pm SEM ($n = 7$).

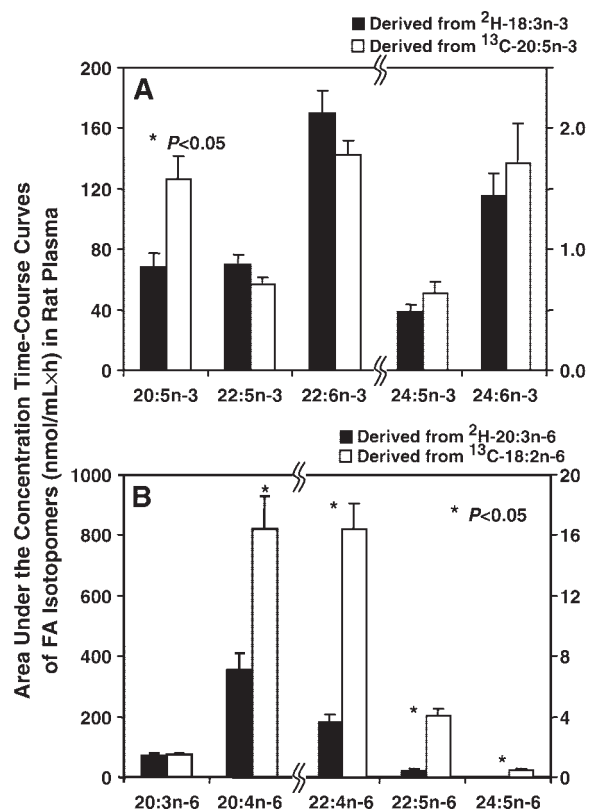


Fig. 6. Accumulation of labeled polyunsaturated fatty acids in rat plasma as the area under the concentration-time course curves (AUC; nmol/ml plasma \times h) of labeled n-3 (A) and n-6 (B) fatty acids, including $^2\text{H}_5$ -20:5n-3, $^2\text{H}_5$ -22:5n-3, and $^2\text{H}_5$ -22:6n-3 derived from $^2\text{H}_5$ -18:3n-3 (closed bars); $^{13}\text{C}_{20}$ -20:5n-3 and $^{13}\text{C}_{20}$ -22:6n-3 derived from ^{13}C -U-20:5n-3 (open bars); $^2\text{H}_5$ -20:4n-6, $^2\text{H}_5$ -22:4n-6, and $^2\text{H}_5$ -22:5n-6 derived from $^2\text{H}_5$ -20:3n-6 (closed bars); and $^{13}\text{C}_{18}$ -20:3n-6, $^{13}\text{C}_{18}$ -20:4n-6, $^{13}\text{C}_{18}$ -22:4n-6, and $^{13}\text{C}_{18}$ -22:5n-6 derived from ^{13}C -U-18:2n-6 (open bars). The right y axis applies to 24:5n-3 and 24:6n-3 in part A and to 22:4n-6, 22:5n-6, and 24:5n-6 in part B. Values are expressed as means \pm SEM ($n = 7$).

metabolism was observed for the n-6 PUFA isotopomers (Fig. 6B). For the n-6 family, there were no differences between the two isotopomers with respect to the AUCs for 20:3n-6, but 20:4n-6, 22:4n-6, and 22:5n-6 showed a much greater ($P < 0.05$) AUC for the ^{13}C -labeled substrates.

Comparison of metabolic end products on a dosage basis

The amount of each fatty acid isotopomer was calculated for the whole plasma compartment and then expressed as a percentage of the initial dose of its respective precursor, so the time course curves allow a more direct comparison (Fig. 7). Although a much greater dosage of the C18 precursor was given, a much greater response was observed for the ^{13}C -20:5n-3-derived 22:6n-3 than for that derived from $^2\text{H}_5$ -18:3n-3, once related to a per dosage basis (Fig. 7A). When the maximal values (D_{\max} ; Table 2) were compared for the 22:6n-3 derived from the two precursors, an 11-fold greater value (0.56) for the 20:5n-3-derived compound to that of the 18:3n-3-derived compound (0.05) was observed. Similarly, for the n-6 fatty acids, this type of plot indicated a much greater response for the C20-derived

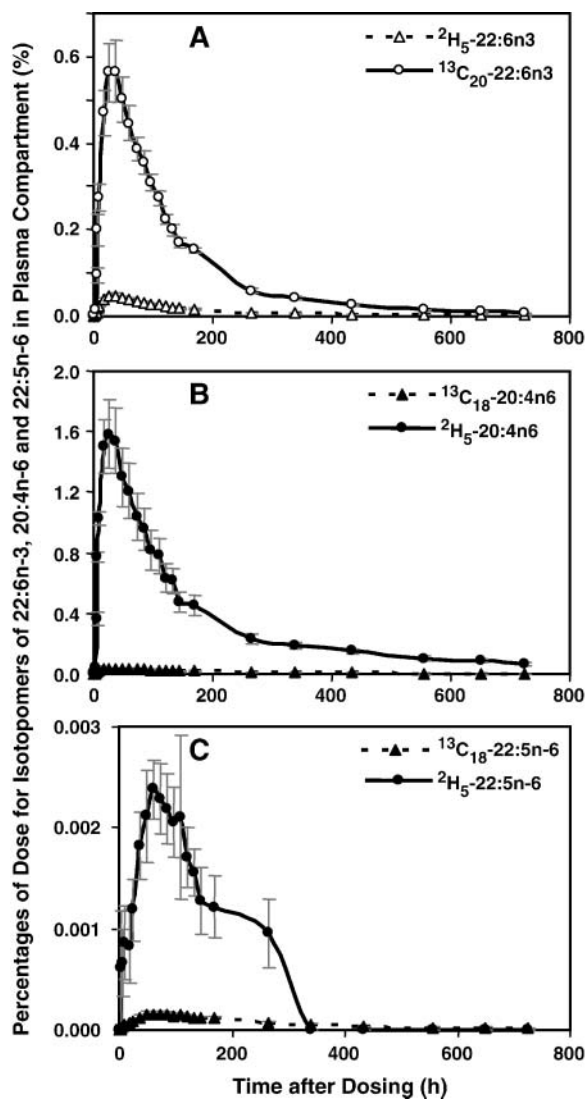


Fig. 7. Time course curves of fatty acids expressed as the percentage of the dose of labeled fatty acids in rat plasma as a function of postdosing time over 30 days for the n-3 end products $^2\text{H}_5$ -22:6n-3 (open triangles) and $^{13}\text{C}_{20}$ -22:6n-3 (open circles) (A), and the n-6 intermediate $^2\text{H}_5$ -20:4n-6 (closed circles) and $^{13}\text{C}_{18}$ -20:4n-6 (closed triangles) (B). Time course curves over 11 days for the n-6 end products $^2\text{H}_5$ -22:5n-6 (closed circles) and $^{13}\text{C}_{18}$ -22:5n-6 (closed triangles) (C).

metabolites with respect to those of the C18 precursors. The curves for both 20:4n-6 and 22:5n-6 were much greater for the $^2\text{H}_5$ -20:3n-6-derived precursor when expressed in this manner. The D_{max} values were 1.6 versus 0.03 for 20:4n-6 derived from $^2\text{H}_5$ -20:3n-6 versus that from $^{13}\text{C}_{18}$ -2n-6 (Table 2), a 48-fold difference. Also, 22:5n-6 derived from $^2\text{H}_5$ -20:3n-6 had a 16-fold greater D_{max} value than when derived from $^{13}\text{C}_{18}$ -2n-6 (0.0024 vs. 0.00015; Table 2).

DISCUSSION

The main finding in this stable isotope tracer study was that more labeled 22:6n-3 was produced from ^{13}C -U-20:5n-3

than from $^2\text{H}_5$ -18:3n-3 when the concentration-time course curves were related to the initial precursor dosage, and more labeled 20:4n-6 and 22:5n-6 were produced from $^2\text{H}_5$ -20:3n-6 than from ^{13}C -U-18:2n-6 when expressed in a similar manner. When the data are expressed in this way, the differences are an order of magnitude or more in favor of the C20 intermediates (Fig. 7). Pawlosky et al. (42, 43) performed a physiological compartmental modeling analysis with deuterium-labeled 18:3n-3 in adults. Using this model, they calculated that only $\sim 0.3\%$ of the 18:3n-3 dose appeared in the plasma and only 0.2% of the total amount of labeled 18:3n-3 in plasma was converted to 20:5n-3. Thus, the overall efficiency of 18:3n-3 conversion to 20:5n-3 and longer chain n-3 metabolites is very low. However, they also calculated that $\sim 63\%$ of the plasma 20:5n-3 was accessible for the production of 22:5n-3 and 37% of the 22:5n-3 was available for the synthesis of 22:6n-3 (42). Those data support the present observations that 20:5n-3 and 20:3n-6 are more efficiently converted to 22:6n-3 and 20:4n-6, respectively, than the C18 precursors. Our data are also consistent with the greater efficacy of the C20 EFAs for altering the tissue highly unsaturated fatty acid composition compared with the C18 precursors. Marzo et al. (44) previously compared radioactive 18:3n-3 and 20:5n-3 metabolism with that of 22:6n-3 in cultured retinoblastoma cells.

Apparent preferential metabolism

The pair of n-3 isotopomers seemed to have fairly similar rates of entry to and exit from the various C22 n-3 pools, with the exception that the ^{13}C -20:5n-3 exits the plasma compartment with a half-time of 7 h and the ^2H -20:5n-3 has a half-time of 14 h (Fig. 3A). However, the entry and exit of the two n-6 20:3n-6 isotopomers differed appreciably: ^2H -20:3n-6 appeared rapidly in plasma and then disappeared with a several-fold faster half-life than ^{13}C -20:3n-6 produced from ^{13}C -18:2n-6 (9 vs. 31 h; Fig. 4A).

Although the simplest hypothesis may have been an expectation that the ^2H - and ^{13}C -tracers would mix in a similar manner within the same endogenous pools, the apparent differential metabolism indicates that carbon atoms entering n-6 metabolism as 18:2n-6 or 20:3n-6 in rat may have different compartmentalization of the precursors and their metabolites in different tissue lipids. This may be attributable to different turnover rates for the different types of plasma lipids or molecular species that carry the two isotopomers. Nevertheless, the general pattern of enrichment values over time (Table 2) follows that expected for the flow of both isotopes through the intermediates along the recognized pathways. The greater progressive loss of enrichment in the n-6 pathway compared with that in the n-3 pathway may reflect larger intermediate pools of n-6 than n-3, which result from the greater proportions of n-6 precursors provided in the maintenance diet.

In addition to these kinetic differences between the C20 precursors and their isotopomers and the C18 precursors, differences were also seen in the successive elongated and desaturated metabolites, in particular in the n-6 family. Several interesting features were apparent upon observing the AUC data. When the first step of metabo-

lism after the introduction of the C20 isotope was inspected (Fig. 6), there appeared to be a relatively greater AUC response for metabolites that originated from the C18 precursor. That is, there was a greater AUC for ^{13}C -20:5n-3 than for ^2H -20:5n-3 ($P < 0.05$), so a greater amount of the ^{13}C -22:5n-3 would be expected. However, an approximately equal AUC of the two 22:5n-3 isotopomers was produced, indicating a preference for that derived from the $^2\text{H}_5$ -18:3n-3. Similarly, although the AUCs for the two 20:3n-6 isotopes were very similar, a larger response was evident for the AUC of the 20:4n-6 derived from the ^{13}C -labeled precursor. This effect may be attributed at least in part to the apparent inefficient use of the precursors during their initial absorption phase. That is, there appear to be fewer C20 molecules routed into the fatty acid anabolic pathways relative to newly synthesized 20:5n-3 or 20:3n-6 molecules, perhaps because of greater catabolism during absorption (45). It is interesting, however, that in the subsequent metabolism of 20:4n-6 to 22:4n-6, the ^{13}C compound was again formed preferentially with respect to the $^2\text{H}_5$ compound (Fig. 4C). It appeared then that 20:4n-6 substrate was more efficiently elongated when it had a history of sequential elongation/desaturation (i.e., ^{13}C -20:4n-6 derived from ^{13}C -18:2n-6) than when it had more recently entered the metabolic pathway. This is consistent with previous reports of a channeling concept for coupled fatty acid elongation/desaturation systems (46), perhaps by a multienzyme complex (47).

Different lipid classes

One possible explanation for these results would be the initial differential incorporation of labeled 18:2n-6 and 20:3n-6 or 18:3n-3 and 20:5n-3 or their metabolites into different lipid classes. A dietary study conducted by Gibson et al. (48) showed that triglycerides (TG) carried most of the 18:3n-3 and part of the 18:2n-6, whereas phospholipids (PL) and cholesteryl esters (CE) retained approximately half of the 18:2n-6. 20:5n-3 was preferentially carried in the CE fraction in rats regardless of whether it originated from endogenous metabolism or from dietary intake. Similarly, 20:4n-6 was predominant in the CE fraction irrespective of the dietary fat source. A study conducted by Morise et al. (20) showed that ~45% of the long-chain PUFAs, primarily of the n-6 family, were localized in PLs, and only a small amount of 18:3n-6 and 20:3n-6 accumulated (49–51).

Similar compartmental effects were observed in isotope tracer studies with EFAs. Different turnover kinetics in different lipid classes was noted by Emken, Adlof, and Gulley (52), who reported that 18:2n-6 was preferentially incorporated into phosphatidylcholine (PC) rather than TG. In other stable isotope studies, ^{13}C -18:3n-3 appeared high in TG in men (53), whereas its metabolites 20:5n-3, 22:5n-6, and 22:6n-3 were high in PL at a later time after dosing. $^2\text{H}_4$ -20:3n-6 incorporated into TG at an early time after administration and later appeared in PL, reaching a peak at 12 h, whereas its metabolite, ^2H -20:4n-6, occurred very little in TG but was primarily found in PL (11, 12). Wijendran et al. (54) observed that PL- ^{13}C -U-20:4n-6 was prefer-

entially incorporated into brain 20:4n-6 in the baboon neonate with respect to the TG- ^{13}C -U-20:4n-6. Similarly, an in vitro study of cultured lung fibroblasts using ^{14}C -labeled fatty acids showed that 20:3n-6, 20:4n-6, and 20:5n-3 were incorporated somewhat differentially into various PL classes, with 20:3n-6 enriched in phosphatidylethanolamine (PE) and phosphatidylglycerol, 20:5n-3 enriched in PC, PE, and phosphatidylinositol (PI), and 20:4n-6 enriched in PC (55). In rat liver microsomes (56, 57), 18:2n-6 was enriched in PC and PE, 20:3n-6 was incorporated mainly into PC, PE, and PI, and 20:4n-6 occurred primarily in PI, whereas C22 fatty acids (i.e., 22:4n-6, 22:5n-6, 22:5n-3, and 22:6n-3) were enriched in PE. In pig microsomes, 20:5n-3 was found mainly in PC (58).

In our study, pilot data of the lipid class distribution in rat plasma at 24 h after giving the four isotopic precursors were collected. Approximately 65% of $^2\text{H}_5$ -18:3n-3 was recovered in TG; however, ^{13}C -20:5n-3 was found primarily in CE (65%). PL (40%) and CE (32%) were the main classes for both the precursor ^{13}C -18:2n-6 and ^2H -18:2n-6 retroconverted from ^2H -20:3n-6. However, ^2H -20:3n-6 was found in NEFA (31%) and PL (48%). Thus, the initial incorporation of the two n-3 and the two n-6 precursors reflects a different lipid class profile, with the precursor having a preference for the lipid classes indicated: $^2\text{H}_5$ -18:3n-3 in TG, ^{13}C -U-20:5n-3 in CE, ^{13}C -18:2n-6 in PL and CE, and $^2\text{H}_5$ -20:3n-6 in PL and NEFA. These studies suggest that differences in the initial lipid class distribution of the various precursors could play an important role in the transport and metabolism of a particular isotope.

Isotope effect


One possible explanation for the differential metabolism of C18 and C20 tracers might involve isotope effects in which ^2H -labeled compounds behave differently from ^{13}C -labeled compounds. A direct comparison of $^2\text{H}_5$ -18:3n-3 and ^{13}C -U-18:3n-3 as well as $^2\text{H}_5$ -18:2n-6 and ^{13}C -U-18:2n-6 in the accompanying paper (36) found little difference between the amounts of $^2\text{H}_5$ -18:3n-3 and ^{13}C -U-18:3n-3, $^2\text{H}_5$ -18:2n-6 and ^{13}C -U-18:2n-6, and their major metabolites $^2\text{H}_5$ -22:6n-3 and $^{13}\text{C}_{18}$ -22:6n-3, $^2\text{H}_5$ -20:4n-6 and $^{13}\text{C}_{18}$ -20:4n-6 in rat plasma at 24 h after rats were given the isotopic tracers simultaneously. Thus, this explanation for the behavior of the various isotopes appears unlikely.

Retroconversion

Retroconversion of $^2\text{H}_5$ -20:3n-6 to $^2\text{H}_5$ -18:3n-6 and $^2\text{H}_5$ -18:2n-6 was observed in this in vivo study. This is consistent with previous in vitro observations (41, 59–62) and also with the in vivo study of Emken et al. (13) concerning the retroconversion of 20:3n-6 to 18:3n-6 and 18:2n-6 in human subjects.

Method advantages and additional applications

This study presents a new methodological approach for using the multiple stable isotope tracer technique for the in vivo study of EFA metabolism. It is demonstrated that four different isotopes may be studied simultaneously using this MESSI technique. An advantage of performing

experiments by this method is that fewer experimental animals or human subjects can be used, because experimental conditions are identical for longitudinal comparisons of the metabolism of different metabolic precursors over time. This approach was used to interpret the flow of EFAs among metabolite pools in animals equilibrated and maintained with steady dietary inputs similar to those commonly used (and similar to typical dietary inputs in the United States). The method can have a wider application in studies of both EFA and NEFA metabolism and also in studies in which dietary variables are introduced. It should be particularly important where sampling must be limited, such as in studies of human infants. 

The authors acknowledge Drs. Lee Chedester and Raouf Kechrid for their advice and expert assistance with animal procedures, Sharon Majchrzak for expert assistance with isotope purification and Dr. William E. M. Lands for his valuable suggestions for revision of the manuscript. This project was funded by the Intramural Research Program of the National Institute on Alcohol Abuse and Alcoholism, National Institutes of Health.

REFERENCES

- Dayton, S., S. Hashimoto, W. Dixon, and M. L. Pearce. 1966. Composition of lipids in human serum and adipose tissue during prolonged feeding of a diet high in unsaturated fat. *J. Lipid Res.* **7**: 103–111.
- Manku, M. S., N. Morse-Fisher, and D. F. Horrobin. 1988. Changes in human plasma essential fatty acid levels as a result of administration of linoleic acid and gamma-linolenic acid. *Eur. J. Clin. Nutr.* **42**: 55–60.
- Lasserre, M., F. Mendy, D. Spielmann, and B. Jacotot. 1985. Effects of different dietary intake of essential fatty acids on C20:3 omega 6 and C20:4 omega 6 serum levels in human adults. *Lipids.* **20**: 227–233.
- Marcel, Y. L., K. Christiansen, and R. T. Holman. 1968. The preferred metabolic pathway from linoleic acid to arachidonic acid in vitro. *Biochim. Biophys. Acta.* **164**: 25–34.
- Sprecher, H. 1986. Comparison of omega-3 and omega-6 fatty acid metabolism. In *Health Effects of Polyunsaturated Fatty Acids in Seafoods*. A. P. Simopoulos, R. R. Kifer, and R. E. Martin, editors. Academic Press, New York. 353–379.
- Hassam, A. G., A. J. Sinclair, and M. A. Crawford. 1975. The incorporation of orally fed radioactive gamma-linolenic acid and linoleic acid into the liver and brain lipids of suckling rats. *Lipids.* **10**: 417–420.
- Demmelair, H., M. Baumheuer, B. Koletzko, K. Dokoupil, and G. Kratl. 1998. Metabolism of U¹³C-labeled linoleic acid in lactating women. *J. Lipid Res.* **39**: 1389–1396.
- Cho, H. P., M. Nakamura, and S. D. Clarke. 1999. Cloning, expression, and fatty acid regulation of the human delta-5 desaturase. *J. Biol. Chem.* **274**: 37335–37339.
- Tang, C., H. P. Cho, M. T. Nakamura, and S. D. Clarke. 2003. Regulation of human delta-6 desaturase gene transcription: identification of a functional direct repeat-1 element. *J. Lipid Res.* **44**: 686–695.
- Stone, K. J., A. L. Willis, W. M. Hart, S. J. Kirtland, P. B. Kernoff, and G. P. McNicol. 1979. The metabolism of dihomogamma-linolenic acid in man. *Lipids.* **14**: 174–180.
- el Boustani, S., B. Descomps, L. Monnier, J. Warnant, F. Mendy, and A. Crastes de Paulet. 1986. In vivo conversion of dihomogamma linolenic acid into arachidonic acid in man. *Prog. Lipid Res.* **21**: 67–71.
- el Boustani, S., J. E. Causse, B. Descomps, L. Monnier, F. Mendy, and A. Crastes de Paulet. 1989. Direct in vivo characterization of delta 5 desaturase activity in humans by deuterium labeling: effect of insulin. *Metabolism.* **38**: 315–321.
- Emken, E. A., R. O. Adlof, S. M. Duval, and G. J. Nelson. 1997. In-

- fluence of dietary arachidonic acid on metabolism in vivo of 8cis,11cis,14-eicosatrienoic acid in humans. *Lipids.* **32**: 441–448.
- Mohrhauer, H., and R. T. Holman. 1963. The effect of dose level of essential fatty acids upon fatty acid composition of the rat liver. *J. Lipid Res.* **58**: 151–159.
- Hirai, A., T. Terano, H. Saito, and Y. Tamura. 1989. Omega-3 fatty acids: epidemiological and clinical aspects. In *Current Topics in Nutrition and Disease: New Protective Roles for Selected Nutrients*. G. A. Spiller and J. Scala, editors. Alan R. Liss, New York. 229–252.
- Mantzioris, E., M. J. James, R. A. Gibson, and L. G. Cleland. 1994. Dietary substitution with an alpha-linolenic acid-rich vegetable oil increases eicosapentaenoic acid concentrations in tissues. *Am. J. Clin. Nutr.* **59**: 1304–1309.
- Hansen, J. B., S. Grimsgaard, H. Nilsen, A. Nordoy, and K. H. Bonaa. 1998. Effects of highly purified eicosapentaenoic acid and docosahexaenoic acid on fatty acid absorption, incorporation into serum phospholipids and postprandial triglyceridemia. *Lipids.* **33**: 131–138.
- Li, D., N. J. Mann, and A. J. Sinclair. 1999. Comparison of n-3 polyunsaturated fatty acids from vegetable oils, meat, and fish in raising platelet eicosapentaenoic acid levels in humans. *Lipids.* **34** (Suppl.): 309.
- Li, D., A. Sinclair, A. Wilson, S. Nakkote, F. Kelly, L. Abedin, N. Mann, and A. Turner. 1999. Effect of dietary alpha-linolenic acid on thrombotic risk factors in vegetarian men. *Am. J. Clin. Nutr.* **69**: 872–882.
- Morise, A., N. Combe, C. Boue, P. Legrand, D. Catheline, B. Delplanque, E. Fenart, P. Weill, and D. Hermier. 2004. Dose effect of alpha-linolenic acid on PUFA conversion, bioavailability, and storage in the hamster. *Lipids.* **39**: 325–334.
- Gibson, R. A., M. A. Neumann, and M. Makrides. 1998. The effects of diets rich in gamma-linolenic acid on plasma fatty acid profiles in term infants. In *Lipids in Infant Nutrition*. Y.-S. Huang and A. J. Sinclair, editors. AOCS Press, Champaign, IL. 19–28.
- Ward, G. R., Y. S. Huang, H. C. Xing, E. Bobik, I. Wauben, N. Auestad, M. Montalto, and P. E. Wainwright. 1999. Effects of gamma-linolenic acid and docosahexaenoic acid in formulae on brain fatty acid composition in artificially reared rats. *Lipids.* **34**: 1057–1063.
- Emken, E. A., W. K. Rohwedder, and H. J. Dutton. 1976. Dual-labeled technique for human lipid metabolism studies using deuterated fatty acid isomers. *Lipids.* **11**: 135–142.
- Emken, E. A., S. Abraham, and C. Y. Lin. 1987. Metabolism of cis-12-octadecenoic acid and trans-9,trans-12-octadecadienoic acid and their influence on lipogenic enzyme activities in mouse liver. *Biochim. Biophys. Acta.* **919**: 111–121.
- Sauerwald, T. U., D. L. Hachey, C. L. Jensen, H. Chen, R. E. Anderson, and W. C. Heird. 1997. Intermediates in endogenous synthesis of C22:6 omega 3 and C20:4 omega 6 by term and preterm infants. *Pediatr. Res.* **41**: 183–187.
- Salem, N., Jr., B. Wegher, P. Mena, and R. Uauy. 1996. Arachidonic and docosahexaenoic acids are biosynthesized from their 18-carbon precursors in human infants. *Proc. Natl. Acad. Sci. USA.* **93**: 49–54.
- Burdge, G. C., and S. A. Wootton. 2002. Conversion of alpha-linolenic acid to eicosapentaenoic, docosapentaenoic and docosahexaenoic acids in young women. *Br. J. Nutr.* **88**: 411–420.
- Vermunt, S. H., R. P. Mensink, M. M. Simonis, and G. Hornstra. 2000. Effects of dietary alpha-linolenic acid on the conversion and oxidation of ¹³C-alpha-linolenic acid. *Lipids.* **35**: 137–142.
- Hoffman, D. R., J. C. DeMar, W. C. Heird, D. G. Birch, and R. E. Anderson. 2001. Impaired synthesis of DHA in patients with X-linked retinitis pigmentosa. *J. Lipid Res.* **42**: 1395–1401.
- Carnielli, V. P., D. J. Wattimena, I. H. Luijendijk, A. Boerlage, H. J. Degenhart, and P. J. Sauer. 1996. The very low birth weight premature infant is capable of synthesizing arachidonic and docosahexaenoic acids from linoleic and linolenic acids. *Pediatr. Res.* **40**: 169–174.
- Su, H. M., L. Bernardo, M. Mirmiran, X. H. Ma, T. N. Corso, P. W. Nathanielsz, and J. T. Brenna. 1999. Bioequivalence of dietary alpha-linolenic and docosahexaenoic acids as sources of docosahexaenoate accretion in brain and associated organs of neonatal baboons. *Pediatr. Res.* **45**: 87–93.
- Lin, Y. H., and N. Salem, Jr. 2002. A technique for the in vivo study of multiple stable isotope-labeled essential fatty acids. *Prostaglandins Leukot. Essent. Fatty Acids.* **67**: 141–146.
- Reeves, P. G., F. H. Nielsen, and G. C. Fahey, Jr. 1993. AIN-93 puri-

- fied diets for laboratory rodents: final report of the American Institute of Nutrition ad hoc writing committee on the reformulation of the AIN-76A rodent diet. *J. Nutr.* **123**: 1939–1951.
34. Furuhashi, K., and T. Onodera. 1983. A simple technique for repeated blood collection from the tail vein of the rat. *J. Toxicol. Sci.* **8**: 161–163.
35. Pawlosky, R. J., H. W. Sprecher, and N. Salem, Jr. 1992. High sensitivity negative ion GC-MS method for detection of desaturated and chain-elongated products of deuterated linoleic and linolenic acids. *J. Lipid Res.* **33**: 1711–1717.
36. Lin, Y. H., R. J. Pawlosky, and N. Salem, Jr. 2005. Simultaneous quantitative determination of deuterium- and carbon-13-labeled essential fatty acids in rat plasma. *J. Lipid Res.* **46**: 1974–1982.
37. Salem, N., Jr., M. Reyzer, and J. Karanian. 1996. Losses of arachidonic acid in rat liver after alcohol inhalation. *Lipids*. **31 (Suppl.)**: 153–156.
38. Yeh, K. C., and K. C. Kwan. 1978. A comparison of numerical integrating algorithms by trapezoidal, Lagrange, and spline approximation. *J. Pharmacokinetic. Biopharm.* **6**: 79–98.
39. Retterstol, K., T. B. Haugen, and B. O. Christophersen. 2000. The pathway from arachidonic to docosapentaenoic acid (20:4n-6 to 22:5n-6) and from eicosapentaenoic to docosahexaenoic acid (20:5n-3 to 22:6n-3) studied in testicular cells from immature rats. *Biochim. Biophys. Acta.* **1483**: 119–131.
40. Food and Drug Administration. 2002. Bioavailability and Bioequivalence Studies for Orally Administered Drug Products—General Considerations. Draft Guidance for Industry.
41. Voss, A., M. Reinhart, S. Sankarappa, and H. Sprecher. 1991. The metabolism of 7,10,13,16,19-docosapentaenoic acid to 4,7,10,13,16,19-docosahexaenoic acid in rat liver is independent of a 4-desaturase. *J. Biol. Chem.* **266**: 19995–20000.
42. Pawlosky, R. J., J. R. Hibbeln, J. A. Novotny, and N. Salem, Jr. 2001. Physiological compartmental analysis of alpha-linolenic acid metabolism in adult humans. *J. Lipid Res.* **42**: 1257–1265.
43. Pawlosky, R. J., J. R. Hibbeln, Y. H. Lin, S. Goodson, P. Riggs, N. Sebring, G. L. Brown, and N. Salem, Jr. 2003. Effects of beef- and fish-based diets on the kinetics of n-3 fatty acid metabolism in human subjects. *Am. J. Clin. Nutr.* **77**: 565–572.
44. Marzo, I., M. A. Alava, A. Pineiro, and J. Naval. 1996. Biosynthesis of docosahexaenoic acid in human cells: evidence that two different delta 6-desaturase activities may exist. *Biochim. Biophys. Acta.* **1301**: 263–272.
45. Menard, C. R., K. J. Goodman, T. N. Corso, J. T. Brenna, and S. C. Cunnane. 1998. Recycling of carbon into lipids synthesized de novo is a quantitatively important pathway of alpha-[U-¹³C]linolenate utilization in the developing rat brain. *J. Neurochem.* **71**: 2151–2158.
46. Infante, J. P., and V. A. Huszagh. 1998. Analysis of the putative role of 24-carbon polyunsaturated fatty acids in the biosynthesis of docosapentaenoic (22:5n-6) and docosahexaenoic (22:6n-3) acids. *FEBS Lett.* **431**: 1–6.
47. Infante, J. P., C. L. Tschanz, N. Shaw, A. L. Michaud, P. Lawrence, and J. T. Brenna. 2002. Straight-chain acyl-CoA oxidase knockout mouse accumulates extremely long chain fatty acids from alpha-linolenic acid: evidence for runaway carousel-type enzyme kinetics in peroxisomal beta-oxidation diseases. *Mol. Genet. Metab.* **75**: 108–119.
48. Gibson, R. A., M. J. James, M. A. Neumann, J. S. Hawkes, and L. G. Cleland. 1992. Incorporation of dietary oleate, linoleate, alpha-linolenate and eicosapentaenoate into the plasma lipid fractions of four strains of rat. *Biochim. Biophys. Acta.* **1126**: 49–52.
49. Sprecher, H. 2001. Differences in the regulation of the biosynthesis and esterification of 20- versus 22-carbon polyunsaturated fatty acids. *World Rev. Nutr. Diet.* **88**: 190–195.
50. Bernert, J. T., Jr., and H. Sprecher. 1975. Studies to determine the role rates of chain elongation and desaturation play in regulating the unsaturated fatty acid composition of rat liver lipids. *Biochim. Biophys. Acta.* **398**: 354–363.
51. Lands, W. E., M. Inoue, Y. Sugiura, and H. Okuyama. 1982. Selective incorporation of polyunsaturated fatty acids into phosphatidylcholine by rat liver microsomes. *J. Biol. Chem.* **257**: 14968–14972.
52. Emken, E. A., R. O. Adlof, and R. M. Gulley. 1994. Dietary linoleic acid influences desaturation and acylation of deuterium-labeled linoleic and linolenic acids in young adult males. *Biochim. Biophys. Acta.* **1213**: 277–288.
53. Burdige, G. C., A. E. Jones, and S. A. Wootton. 2002. Eicosapentaenoic and docosapentaenoic acids are the principal products of alpha-linolenic acid metabolism in young men. *Br. J. Nutr.* **88**: 355–363.
54. Wijendran, V., M. C. Huang, G. Y. Diau, G. Boehm, P. W. Nathanielsz, and J. T. Brenna. 2002. Efficacy of dietary arachidonic acid provided as triglyceride or phospholipid as substrates for brain arachidonic acid accretion in baboon neonates. *Pediatr. Res.* **51**: 265–272.
55. Weithmann, K. U., H. Peterson, and A. Sevanian. 1989. Incorporation of arachidonic, dihomogamma linolenic and eicosapentaenoic acids into cultured V79 cells. *Lipids*. **24**: 173–178.
56. Garda, H. A., A. M. Bernasconi, M. A. Tricerri, and R. R. Brenner. 1997. Molecular species of phosphoglycerides in liver microsomes of rats fed a fat-free diet. *Lipids*. **32**: 507–513.
57. Shimada, Y., T. Morita, and K. Sugiyama. 2003. Dietary eritadenine and ethanolamine depress fatty acid desaturase activities by increasing liver microsomal phosphatidylethanolamine in rats. *J. Nutr.* **133**: 758–765.
58. Menguy, L., R. Christon, A. Van Dorsselaer, and C. L. Leger. 1992. Apparent relative retention of the phosphatidylethanolamine molecular species 18:0–20:5(n-3), 16:0–22:6(n-3) and the sum 16:0–20:4(n-6) plus 16:0–20:3(n-9) in the liver microsomes of pig on an essential fatty acid deficient diet. *Biochim. Biophys. Acta.* **1123**: 41–50.
59. Verdino, B., M. L. Blank, O. S. Privett, and W. O. Lundberg. 1964. Metabolism of 4,7,10,13,16-docosapentaenoic acid in the essential fatty acid-deficient rat. *J. Nutr.* **83**: 234–238.
60. Sprecher, H. 1967. The total synthesis and metabolism of 7,10,13,16-docosatetraenoate in the rat. *Biochim. Biophys. Acta.* **144**: 296–304.
61. Schlenk, H., J. L. Gellerman, and D. M. Sand. 1967. Retroconversion of polyunsaturated fatty acids in vivo by partial degradation and hydrogenation. *Biochim. Biophys. Acta.* **137**: 420–426.
62. Schlenk, H., D. M. Sand, and J. L. Gellerman. 1969. Retroconversion of docosahexaenoic acid in the rat. *Biochim. Biophys. Acta.* **187**: 201–207.